




# Prospects for beam-based study of dodecapole nonlinearities in the CERN High-Luminosity Large Hadron Collider

E. H. Maclean<sup>1,2,a</sup> , F. S. Carlier<sup>1,3</sup>, J. Dilly<sup>1,4</sup>, M. Le Garrec<sup>1,5</sup>, M. Giovannozzi<sup>1</sup>, R. Tomás<sup>1</sup>

<sup>1</sup> Beams Department, CERN, Meyrin, Switzerland

<sup>2</sup> University of Malta, Msida, Malta

<sup>3</sup> EPFL, Lausanne, Switzerland

<sup>4</sup> Humboldt University of Berlin, Berlin, Germany

<sup>5</sup> Goethe University of Frankfurt, Frankfurt, Germany

Received: 24 February 2022 / Accepted: 6 October 2022  
© The Author(s) 2022

**Abstract** Nonlinear magnetic errors in low- $\beta$  insertions can have a significant impact on the beam-dynamics of a collider, such as the CERN Large Hadron Collider (LHC) and its luminosity upgrade (HL-LHC). Indeed, correction of sextupole and octupole magnetic errors in LHC experimental insertions has yielded clear operational benefits in recent years. Numerous studies predict, however, that even correction of nonlinearities up to dodecapole order will be required to ensure successful exploitation of the HL-LHC. It was envisaged during HL-LHC design that compensation of high-order errors would be based upon correction of specific resonances, as determined from magnetic measurements during construction. Experience at the LHC demonstrated that beam-based measurement and correction of the sextupole and octupole errors was an essential complement to this strategy. As such, significant interest also exists regarding the practicality of beam-based observables of multipoles up to dodecapole order. Based on experience during the LHC's second operational run, the viability of beam-based observables relevant to dodecapole order errors in the experimental insertions of the HL-LHC are assessed and discussed in detail in this paper.

## 1 Introduction

To achieve the desired collision rates in the High-Luminosity Large Hadron Collider (HL-LHC) [1], beam intensities will be significantly increased relative to LHC operation (achieved via upgrades of the injector chain [2]) and optics will be squeezed to significantly smaller  $\beta^*$  in the experimental insertion regions (IRs) than for LHC operation. This latter requirement necessitates large  $\beta$ -functions in nearby elements of the lattice, notably the quadrupole triplets and the separation/recombination dipoles. Nonlinear errors in these insertion magnets can thus significantly perturb the beam dynamics. Control of such IR-errors during design and construction has been an issue of longstanding concern to the collider community, notably at the Tevatron [3], RHIC [4] and LHC [5–8]. Beam-based optimisation of lifetime using nonlinear corrector magnets in the experimental IRs yielded operational benefits at the RHIC collider [9, 10], where measurements of feed-down to tune also showed significant promise for compensation of IR errors [11]. Operational benefits were obtained at the LHC through beam-based compensation of sextupole and octupole errors in the ATLAS and CMS insertions [12]. Control of IR-nonlinearities is also a key ingredient in the design and development of the Future Circular Collider [13–15] and is expected to represent a challenge for operation of SuperKEKB [16].

In the HL-LHC it is proposed to correct IR-errors up to dodecapole order in the experimental insertions [1]. During the HL-LHC design it was envisaged that such corrections would be calculated based upon magnetic measurements performed during construction, following the procedure described in [6, 17]. This nominal correction strategy is heavily dependent on the quality of the magnetic model [18–20]. In practice, at the LHC it was found that discrepancies existed between predictions of the magnetic model of the IR sextupole and octupole errors, and beam-based observations [12, 21]. It is desirable therefore, to have beam-based observables up to dodecapole order which could be used to validate (and if necessary refine) corrections. During its second operational run several sessions of LHC beam-time were devoted to testing beam-based observables with a view to dodecapole measurement in HL-LHC, with further experience gained during regular optics commissioning. The aim of this paper is to present the relevant LHC experience, and assess the viability of the techniques for application in the HL-LHC.

The structure of this paper is as follows: in Sect. 2 notation and assumptions regarding the expected dodecapole errors in the HL-LHC used in the rest of the paper are introduced, while Sect. 3 summarises briefly the main motivations for correction to such high-order. Section 4 discusses the prospect to study dodecapole errors via methods based on amplitude detuning: viability of

<sup>a</sup> e-mail: [ewen.hamish.maclean@cern.ch](mailto:ewen.hamish.maclean@cern.ch) (corresponding author)

measuring quadratic detuning directly generated by dodecapoles is assessed via measurement of artificially introduced sources in the LHC, and LHC experience of measuring feed-down to linear (octupole-like) detuning is reviewed and compared to the expected feed-down in HL-LHC. In Sect. 5 LHC experience of measurement of high-order resonance driving terms is reviewed, and compared to expectations in HL-LHC. Finally Sect. 6 and 7 present the prospect to measure changes in dynamic aperture of free motion and forced-oscillations, due to the dodecapole errors expected in HL-LHC, based upon measurements of artificially introduced sources in the LHC. A technical report providing further details of the studies in this paper is available at [22].

## 2 Expected dodecapole errors in HL-LHC

A key element of the high-luminosity LHC upgrade (HL-LHC) will be replacement of existing triplet quadrupoles with larger aperture magnets, allowing for a baseline optics squeeze to  $\beta^* = 0.15$  m (the LHC currently operates with an ultimate squeeze in the range  $\beta^* = 0.3$  m – 0.25 m). Dodecapole errors in the new HL-LHC triplets are expected to be the dominant source of  $b_6$  in the HL-LHC during operation with squeezed beams. Target values for dodecapole errors in the triplets were initially specified as a systematic value of  $b_6 = -0.64$  units in the body of the magnet together with a random component  $\sigma(b_6) = 1.1$  units, where a dimensionless ‘unit’ of the multipole error ( $b_n$ , of multipole order  $n$ ) is defined relative to the main field of the magnet ( $B_{N,\text{main}}$ , of multipole order  $N$ ) at a reference radius ( $R_{\text{ref}}$ , equal to 0.05 m in the HL-LHC triplets)

$$b_n[\text{unit}] = \frac{B_n}{B_{N,\text{main}}} R_{\text{ref}}^{n-N} \times 10^{-4} \quad (1)$$

where the field gradients ( $B_n$ ) and normalised field strength ( $K_n$ ) are defined

$$\begin{aligned} B_n[\text{Tm}^{1-n}] &= \frac{1}{(n-1)!} \frac{\partial^{n-1} B_y}{\partial x^{n-1}} \\ K_n[\text{m}^{-n}] &= \frac{1}{B\rho} (-1)^n B_n \end{aligned} \quad (2)$$

and  $1/(B\rho)$  is the beam rigidity. Skew multipoles are similarly denoted  $a_n$ . Recent work on the development of HL-LHC triplet magnets suggested dodecapole errors in HL-LHC could exceed the original target [23–25], though significant work is also still underway to improve magnet designs [24, 25]. A more pessimistic expectation of the normal dodecapole errors can be taken to be systematic value of  $b_6 = -4$  units in the body of the magnet, with an unchanged random part ( $\sigma(b_6) = 1.1$  units). Expectation for decapole and lower-order multipoles can be found in [23–25].

## 3 Motivation for correction to dodecapole order in HL-LHC

A major concern over correction of IR-nonlinearities in HL-LHC arises from potential reduction of beam-lifetime and dynamic aperture (DA). DA is defined as the extent of the phase-space volume in which particle motion remains bounded (see, e.g. [26] and references therein for more detailed discussion). Numerous simulation-based studies predict that correction to dodecapole order is necessary to guarantee sufficient DA for effective exploitation of the collider [27–29]. As an example, Fig. 1 shows the reduction to simulated DA after  $10^6$  turns (about 1.5 minutes) if dodecapole errors (with systematic  $b_6 = -4$  units) in the ATLAS and CMS insertion triplets were left uncorrected. Simulation was performed for the baseline HL-LHC configuration at end-of-squeeze ( $\beta^* = 0.15$  m) including the beam-beam interactions, with nominal correction of all other linear and nonlinear errors (following the procedure [17]). Values shown are minimum DA over sixty instances (‘seeds’) of the magnetic model to account for uncertainties in the errors. Failure to correct the normal dodecapole errors leads to a substantial ( $\approx 25\%$ ) reduction in predicted DA which poses a risk to productive operation. The impact of uncorrected dodecapole sources on operation of the HL-LHC with colliding beams has been discussed in detail in [30].

In addition to concerns over dynamic aperture, feed-down from the high-order errors can also represent a challenge to HL-LHC operation. To stabilise non-colliding beams during operation with high intensity, the HL-LHC will operate with amplitude detuning purposefully introduced via Landau octupole magnets in the arcs. Limited margin will be available in the Landau octupole strength to maintain beam-stability while also maintaining sufficient dynamic aperture [31]. Existing estimates [31] anticipate a tolerance on detuning from the IR-errors of  $\approx 12 \times 10^3 \text{ m}^{-1}$ . In the absence of limitation from the cryogenic system, ultimate HL-LHC scenarios foresee collisions beginning from  $\beta^* = 0.4$  m: Fig. 2 shows predictions of linear amplitude dependent tune shifts generated by feed-down from decapole and dodecapole errors in the ATLAS and CMS IRs upon introduction of a  $190 \mu\text{rad}$  crossing-scheme at  $\beta^* = 0.4$  m in the HL-LHC (where the pessimistic estimate of a systematic  $b_6 = -4$  units has been considered). In the absence of correction up to dodecapole order the feed-down to linear amplitude detuning can significantly exceed the expected  $12 \times 10^3 \text{ m}^{-1}$  margin for the Landau octupoles (indicated in purple in Fig. 2), though this issue will be significantly alleviated during early years of HL-LHC operation, and non-ultimate scenarios, by starting collisions at higher  $\beta^*$ .

**Fig. 1** Simulated DA of the HL-LHC in collision at end-of-squeeze ( $\beta^* = 0.15$  m, with beam-beam included), with (blue) and without (red) correction of normal dodecapole errors in the ATLAS and CMS insertion triplets

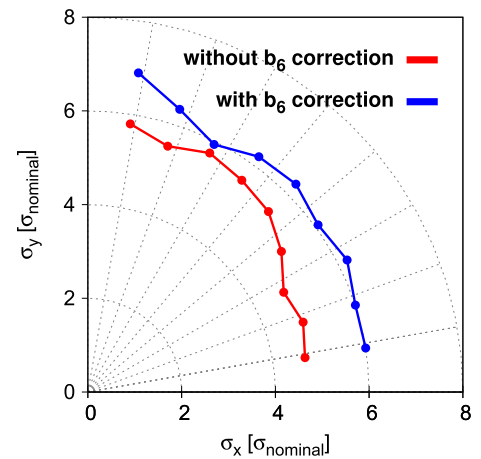


**Fig. 2** Predicted detuning generated by decapole and dodecapole feed-down upon application of 190  $\mu$ rad crossing-scheme in the HL-LHC at  $\beta^* = 0.4$  m. Histograms are shown before (red) and after (green) application of decapole and dodecapole corrections in the ATLAS and CMS insertions. Dodecapole errors are considered for a systematic  $b_6 = -4$  units together with a random component of 1.1 unit

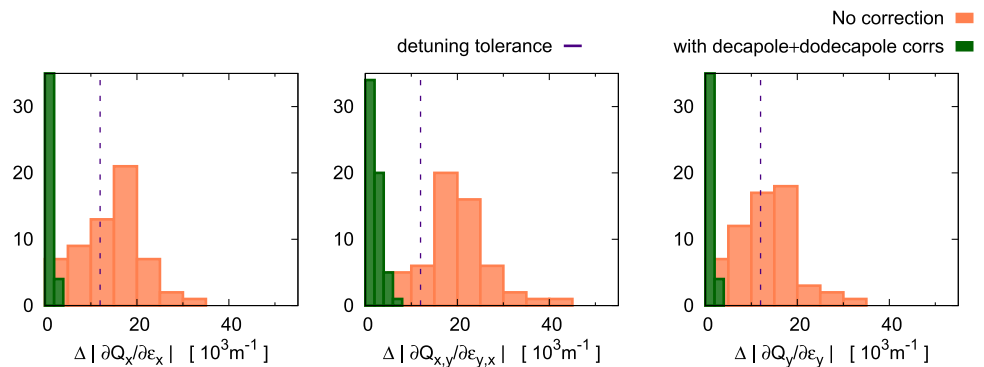
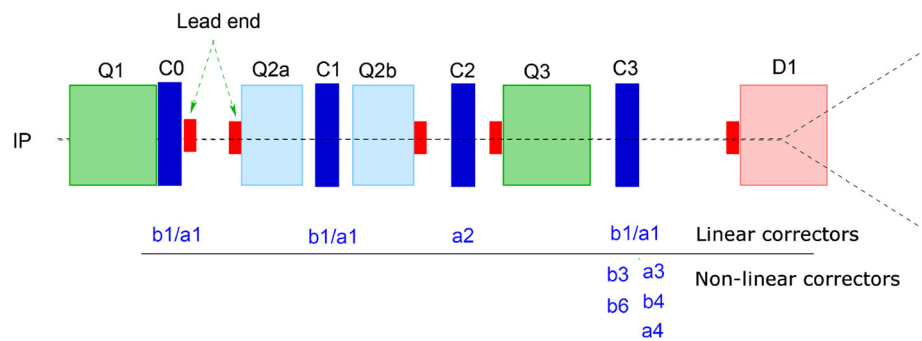


**Fig. 3** Linear and nonlinear corrector layout in LHC experimental IRs [17]



It has also been observed in the LHC that amplitude detuning at the level of  $40 \times 10^3 \text{ m}^{-1}$  caused a substantial degradation to performance of the online tune and coupling measurement [12]. This posed an obstacle even to commissioning of the linear optics in the LHC during 2016 [12] (via techniques such as K-modulation). In the most pessimistic cases considered in Fig. 2 a comparable detuning can be generated through feed-down (increasing for larger crossing-angles and smaller  $\beta^*$  configurations). Maintaining the performance of beam-instrumentation represents a further motivation for correction up to dodecapole order in HL-LHC.

To facilitate local correction of nonlinear errors in the experimental insertions, dedicated correctors are located on the left and right sides of each experimental IR. In the LHC correctors exist for normal/skew sextupole, normal/skew octupole, and normal dodecapole errors. In the HL-LHC additional correctors will be available for normal/skew decapole and skew dodecapole errors. Figure 3 displays a schematic of one side of an LHC experimental IR. The nonlinear correctors in the LHC and HL-LHC are located on the non-IP side of the Q3 triplet quadrupole (location C3 in Fig. 3). Further details regarding the lattice and the corrector magnets may be found in [5, 17, 29, 32]. During several studies presented in this paper dodecapole errors were artificially introduced into the LHC lattice: in all cases this was done using the  $b_6$  correctors in the experimental IRs.

#### 4 Amplitude detuning

Amplitude detuning is the variation of tune as a function of Courant-Snyder invariant ( $\epsilon_{x,y}$ ) or particle action ( $J_{x,y}$ , with  $\epsilon_{x,y} = 2J_{x,y}$ ). It is described as a Taylor expansion about the unperturbed tune,

$$Q_z(\epsilon_x, \epsilon_y) = Q_{z0} + \frac{\partial Q_z}{\partial \epsilon_x} \epsilon_x + \frac{\partial Q_z}{\partial \epsilon_y} \epsilon_y + \frac{1}{2!} \left( \frac{\partial^2 Q_z}{\partial \epsilon_x^2} \epsilon_x^2 + 2 \frac{\partial^2 Q_z}{\partial \epsilon_x \partial \epsilon_y} \epsilon_x \epsilon_y + \frac{\partial^2 Q_z}{\partial \epsilon_y^2} \epsilon_y^2 \right) + \dots \quad (3)$$

where  $z = x, y$ . For the purpose of this paper, terms  $\frac{\partial^{(1)} Q}{\partial \epsilon^{(1)}}$  are denoted as ‘linear detuning coefficients’ and  $\frac{\partial^{(2)} Q}{\partial \epsilon^{(2)}}$  the ‘quadratic detuning coefficients’. Terms as in Eq. (3) which depend only on the horizontal, or only on the vertical planes (e.g.  $\frac{\partial Q_x}{\partial \epsilon_x}$  and  $\frac{\partial Q_y}{\partial \epsilon_y}$ ) are denoted as the ‘direct detuning coefficients’. Terms which depend on both the horizontal and vertical planes (e.g.  $\frac{\partial Q_x}{\partial \epsilon_y} = \frac{\partial Q_y}{\partial \epsilon_x}$ ) are denoted as ‘cross-term detuning coefficients’.

To first-order in the multipole strength a linear detuning is generated by normal octupole fields, and a quadratic detuning by normal dodecapole fields. Higher-order multipoles can contribute to a given detuning order through feed-down: thus a normal dodecapole directly generates quadratic detuning and can generate linear detuning via feed-down to a normal octupole field. Lower-order and skew multipoles may also contribute to a given detuning order through perturbations of higher-order in multipole strength [33]. Beam-based measurement of the high-order multipoles in HL-LHC will only take place after correction of sextupole and octupole errors [34], at which point any contributions from such lower-order multipoles are predicted to be negligible compared to the contribution to linear detuning from feed-down and the contribution to quadratic detuning directly from the dodecapoles.

Amplitude detuning at top energy in the LHC is measured using an AC-dipole, which excites driven oscillations of the beam that can be ramped up and down adiabatically, allowing repeated excitation of the same bunch [35–37]. This is in contrast to measurement via single-kicks which can be employed at injection [38] but is impossible to apply at top-energy due to constraints from machine protection and practical limitations due to bunch decoherence [18]. Detuning measured via AC-dipole differs from that of free oscillations according to a well-defined relation [39], in particular direct detuning coefficients are enhanced by a factor which varies according to the detuning order. Where measured detuning coefficients are quoted in this paper the effect of the driven oscillation has been compensated to give the equivalent free oscillation coefficients. Further detail of the amplitude detuning measurement techniques are provided in [22, 39].

##### 4.1 Quadratic amplitude detuning from normal dodecapoles ( $b_6$ )

Figure 4 shows the magnitude of quadratic detuning anticipated for the HL-LHC at  $\beta^* = 0.15$  m, flat-orbit. Two distributions are shown, for the original target error specification (with systematic  $b_6 = -0.64$  units, blue) and for the more pessimistic estimate based on early magnet designs (with systematic  $b_6 = -4$  units, red). Histograms are shown over sixty instances of the model to account for uncertainties in the errors. The anticipated magnitude of the detuning is dominated by the uncorrected normal-dodecapole errors in the ATLAS and CMS IRs.

Amplitude detuning measurements with AC-dipole have become routine in the LHC at top-energy as a way to study octupole errors [12]. During this time no quadratic variation of the tune shift with amplitude was observed. To test the prospect for measurement of quadratic detuning in HL-LHC therefore, dodecapole correctors in the LHC experimental IRs were used to increase the  $b_6$  content of the ATLAS and CMS insertions during dedicated machine tests at  $\beta^* = 0.4$  m. The four dodecapole correctors were uniformly powered to a strength of  $K_6 = 24\,950 \text{ m}^{-6}$ , generating a predicted quadratic detuning of  $\frac{\partial^2 Q_x}{\partial \epsilon_x^2} = -4.5 \times 10^{12} \text{ m}^{-2}$  (in the LHC at  $\beta^* = 0.4$  m). This quadratic detuning is representative of that anticipated in the HL-LHC at  $\beta^* = 0.15$  m (as seen in Fig. 4). Sextupole and octupole corrections determined during commissioning [12] were applied. A detailed description of the study is found in [40].

Having increased the LHC dodecapole content in this manner, amplitude detuning measurements with AC-dipole were attempted for the horizontal action. Figure 5 shows the outcome of the detuning measurement. Data shown in the plot corresponds to the difference between the natural tune determined from spectral analysis of the AC-dipole excitation, and the unkicked tune measured in the LHC BBQ [41, 42]. In the absence of enhanced  $b_6$ , no second-order detuning is observed in the LHC. With enhanced  $b_6$  however, a quadratic component to the variation of tune with amplitude can be observed.

Table 1 shows the quadratic detuning coefficient and  $\chi_{\text{red}}^2$  statistic determined from fits of the measurement with the enhanced  $b_6$  sources in Fig. 5 (black/red). The expected value from the model is also shown. Attempting to fit the measurement with only a linear detuning returned a  $\chi_{\text{red}}^2$  statistic which was significantly worse than fits including the quadratic term, demonstrating the identification of quadratic detuning with the enhanced  $b_6$  sources.

The measured quadratic detuning agrees with the expected value within the standard error on the fitted coefficient, and within 20% of the expected value. The achievable uncertainty on the measurement of  $\sigma \leq 1 \times 10^{12} \text{ m}^{-2}$  can be compared to the predicted HL-LHC quadratic detuning in Fig. 4, and implies that good precision on the global IR1+IR5  $b_6$  correction should be achievable at end-of-squeeze for the expected dodecapole errors, particularly for scenarios with strong  $b_6$  sources which are of greatest relevance to operation.

**Fig. 4** Predicted quadratic detuning coefficients for the HL-LHC at  $\beta^* = 0.15$  m. Histograms are shown over sixty instances of the model to account for uncertainties in the errors. Two configurations of the systematic part of the normal dodecapole error in the magnet body are considered, the HL-LHC target value (systematic  $b_6 = -0.64$  units, blue) and a more pessimistic expectation based on early magnet designs (systematic  $b_6 = -4$  units, red)

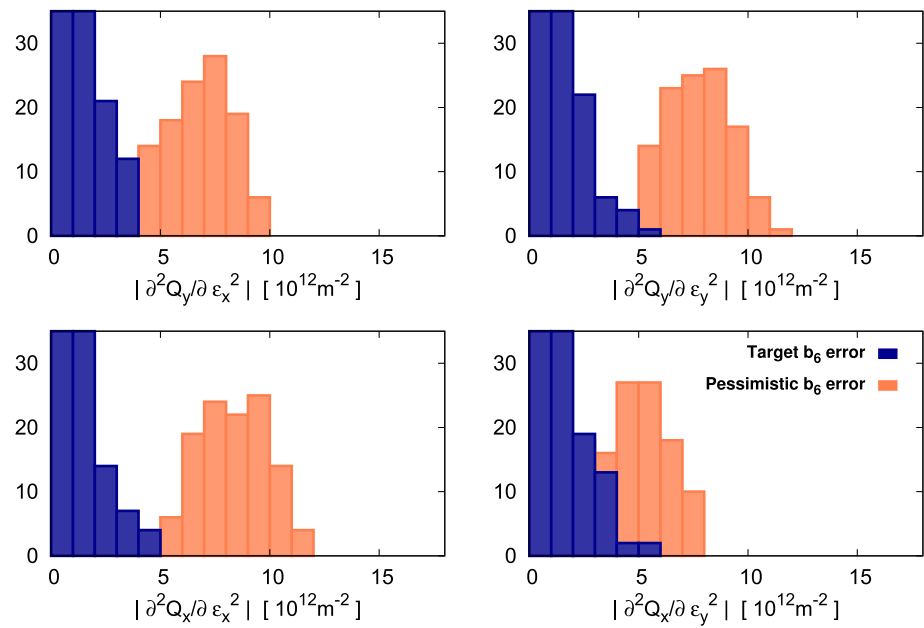


**Fig. 5** Measurement of tune change with action of AC-dipole excitation, with and without an artificially enhanced dodecapole content of the ATLAS and CMS insertions

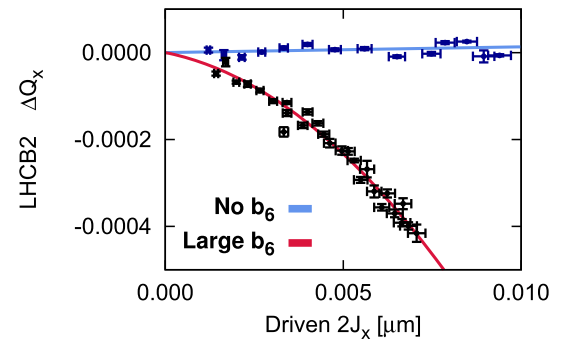


**Table 1** Second-order detuning coefficients and reduced chi-squared statistics obtained from fits to the AC-dipole detuning data. The expected second-order detuning coefficient obtained from PTC\_NORMAL [43] for the applied powering of MCTX is also shown

Fit form	$\chi^2_{red}$	$\partial^2 Q_x / \partial \epsilon_x^2 [10^{12} \text{ m}^{-2}]$
Model	N/A	- 4.5
Linear fit	16.1	0.0
Quadratic fit	5.8	-5.5 ± 1

Conventional detuning measurements based upon single-kicks cannot be applied in the HL-LHC at top energy. The results presented in this section represent a first demonstration of measurement of quadratic detuning with driven oscillations at top energy in the LHC. Results were consistent with predictions of the model for a well defined  $b_6$  source introduced using dodecapole correctors in the ATLAS and CMS insertions. The technique shows sufficient precision to provide a direct quantitative probe for  $b_6$  errors in experimental insertions of the HL-LHC at end-of-squeeze.

#### 4.2 Feed-down to linear amplitude detuning from normal dodecapoles and crossing-angle orbit bumps

Measurement of quadratic detuning described above appears a promising technique, but suffers from two weaknesses. As a global variable it does not distinguish locally between errors in the ATLAS and CMS insertions. Secondly, given the strong scaling of the quadratic detuning with  $(\beta^*)^{-3}$ , it is only expected to be measurable at very low- $\beta^*$ , such as the  $\beta^* = 0.15$  m optics considered in Fig. 4.

Feed-down to linear detuning provides a potential observable for both decapole and normal dodecapole errors, and can overcome some of the weaknesses of a quadratic detuning measurement. Crossing-angles can be varied independently in the IRs providing a

**Fig. 6** Example of amplitude detuning measurements performed for various configurations of the crossing-scheme in the LHC at  $\beta^* = 0.3$  m

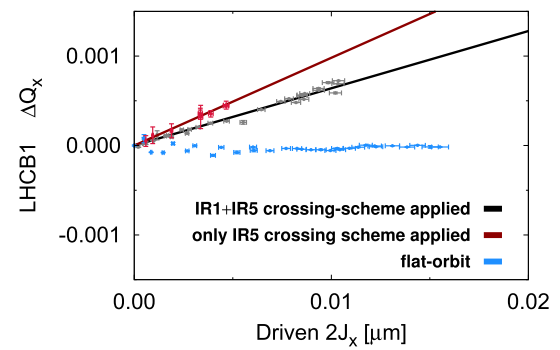
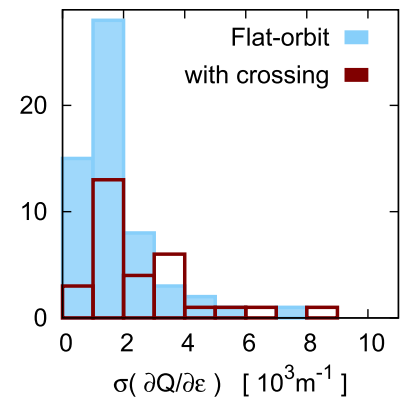


**Table 2** Direct detuning coefficients measured in the LHC at  $\beta^* = 0.3$  m with the full LHC crossing-scheme applied and with only the IR5 crossing-scheme applied

[ $10^3 \text{m}^{-1}$ ]	LHC B1		LHC B2	
	IR1+5	IR5 only	IR1+5	IR5 only
$\partial Q_x / \partial 2J_x$	$+32 \pm 2$	$+46 \pm 3$	$-5 \pm 1$	$+2 \pm 1$
$\partial Q_y / \partial 2J_y$	$-40 \pm 1$	$+5 \pm 2$	$+20 \pm 4$	$+13 \pm 2$

**Fig. 7** Histograms of standard errors on linear detuning coefficients measured in the LHC, measurements performed with flat-orbit (blue) and with some crossing-scheme applied (red)



local observable, and due to weaker scaling with  $(\beta^*)^{-2}$  it may be a viable observable earlier in the HL-LHC squeeze. The feed-down is also of direct operational relevance as discussed in Sect. 3.

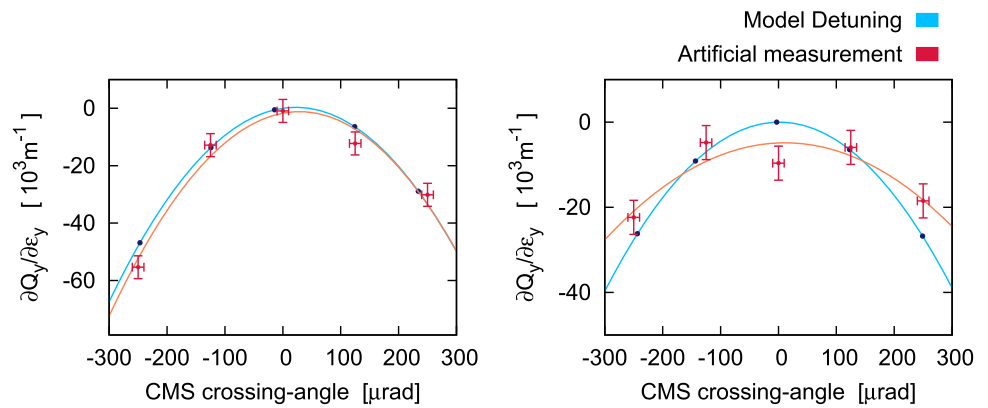
In the LHC multiple measurements of shifts to linear detuning with changes in crossing-scheme have been performed, both to test measurement viability and to study higher-order errors in the existing triplets. An example of one such study is shown in Fig. 6, which shows a detuning measurement performed at flat-orbit (blue), with IR1 and IR5 crossing-angles applied at  $160 \mu\text{rad}$  (black), and with only the crossing-angle in IR5 applied at  $160 \mu\text{rad}$  (red). Measurements were performed in 2018 at  $\beta^* = 0.3$  m. At flat-orbit the detuning is consistent with zero (normal octupole corrections having been applied). Upon application of crossing-angles in the IRs clear shifts to the linear detuning can be observed, indicating the presence of errors of decapole or higher-order in the existing LHC IRs. Table 2 presents the direct detuning coefficients measured with crossing-angle bumps applied in Fig. 6.

Figure 6 and Table 2 illustrate that high-quality measurements of the linear detuning can be performed in the LHC even when large crossing-angles are applied in the IRs, and that feed-down to linear detuning can be measured at high-energy using driven oscillations with an AC-dipole. A review of all detuning measurements performed at top energy in the LHC is provided in [44], and prospects for correction in the LHC are discussed in [45]. Figure 7 presents a histogram of the standard errors obtained from all successful linear detuning measurements performed throughout the LHC’s second Run, for measurements performed at flat-orbit (blue) and with crossing-angles applied in the IRs (red). No distinction is made between measurements of different detuning terms or between the LHC beams since all show comparable measurement uncertainties. Studies performed with a crossing-scheme applied achieved a comparable measurement quality to that obtained at flat-orbit.

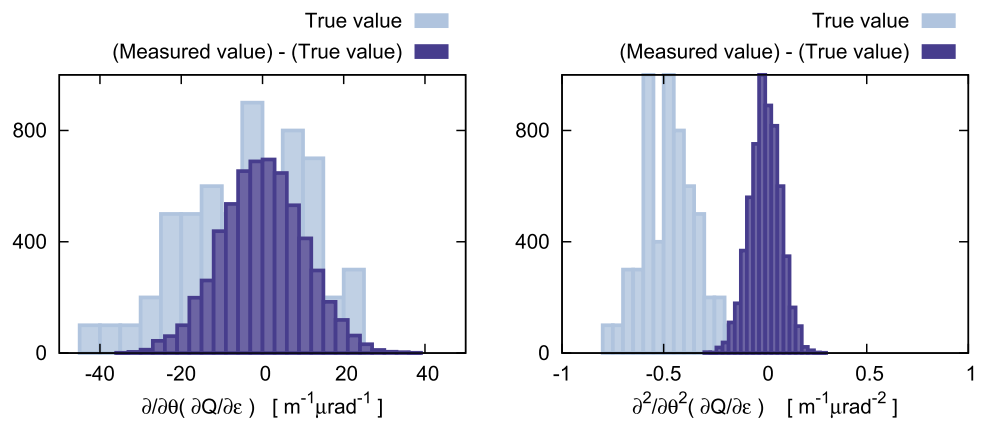
It is desired to extrapolate this LHC experience to the HL-LHC, in order to consider the viability of measuring feed-down to amplitude detuning at both  $\beta^* = 0.4$  m (representing a  $\beta^*$  of operational relevance to the early years of HL-LHC operation) and  $\beta^* = 0.15$  m (end-of-squeeze: where feed-down effects will be most significant). To this end a series of simulated measurements were considered at each  $\beta^*$ .

Each simulated measurement consisted of a scan of the crossing-angle (individually for each IR) over a  $\pm 250 \mu\text{rad}$  range ( $250 \mu\text{rad}$  is the nominal HL-LHC crossing-scheme), with each scan consisting of linear detuning measurements at five different crossing-angles. A total of 6000 simulated scans were performed for each  $\beta^*$  and IR studied. The linear and quadratic variations of

**Fig. 8** Two examples of artificial measurements of linear detuning versus crossing-angle in IR5 at  $\beta^* = 0.4$  m, corresponding to different seeds of the magnetic model, and different random Gaussian errors applied to the individual crossing-angle and detuning values. The true variation of detuning from the PTC model is shown in blue, and the artificial measurement in red



**Fig. 9** Histograms of expected linear (left) and quadratic (right) variations of the vertical direct detuning coefficient as a function of the crossing-angle in IR5, for models of the HL-LHC at  $\beta^* = 0.4$  m (pale blue). The difference between the modelled linear and quadratic variations and those determined from artificial crossing-scan measurements are shown in dark blue



the detuning coefficients were determined from PTC [43] models of the HL-LHC with a systematic  $b_6 = -4$  units and a random  $\sigma_{b_6} = 1.1$  units. Sixty instances (‘seeds’) of the errors were considered to account for the random  $b_6$  component. For each seed of the magnetic model 100 instances of random Gaussian errors were applied to the individual detuning points in each scan (giving the total of 6000 simulated scans). To generate the random errors on the crossing-angle and detuning values at each point in the simulated scans, the LHC precision of the crossing-angle was taken ( $\sigma_{\text{xing}} = 10 \mu\text{rad}$ ), and the precision in the detuning measurement was taken to be  $\sigma_{\text{detuning}} = 4000 \text{ m}^{-1}$  (based on Fig. 7). These values were truncated at  $3\sigma$ . For each of the 6000 scans the linear and quadratic variation of detuning vs crossing-angle was determined from a polynomial fit of the five measurement points and compared to the expected values from the PTC models.

Figure 8 shows two examples of the simulated scans of detuning vs crossing-angle at  $\beta^* = 0.4$  m, corresponding to different seeds of the magnetic model, and different random Gaussian errors applied to the individual crossing-angle and detuning values. The detuning vs crossing-angle in the model is shown in blue, the simulated measurement in red, and polynomial fits to simulated measurements in orange. The left and right plots show particularly good and bad instances of the artificial measurement data, respectively.

Decapole errors can be quantified by the linear variation of detuning with crossing-angle and normal dodecapole errors can be quantified by the quadratic variation. Figure 9 shows histograms over the 6000 simulated scans, of the true linear (left, pale blue) and quadratic (right, pale blue) variations of the vertical direct detuning coefficient with IR5 crossing-angle, as obtained from the PTC models. This can be compared to the difference between the artificially measured and true values (dark blue). Measurement based on feed-down is viable if the measurement discrepancy (dark blue) is small compared to expected value (light blue).

For the decapole (linear) feed-down the distribution of the measurement discrepancy (Fig. 9 left, dark blue) is comparable to the uncorrected value (Fig. 9 left, pale blue). This implies that at  $\beta^* = 0.4$  m the crossing-scan technique lacks sufficient precision to measure the decapole errors. By contrast the measurement discrepancy in the quadratic variation of detuning with crossing-angle (Fig. 9 right, dark blue) is significantly smaller than the expected values (Fig. 9 right, pale blue) for uncorrected dodecapole errors, which implies that at  $\beta^* = 0.4$  m the crossing-scan technique does have sufficient precision to measure the normal dodecapole errors. This reflects that, for this  $\beta^*$  and configuration of the errors, feed-down is dominated by the dodecapole contribution and the decapole contribution is too small to measure reliably.

At  $\beta^* = 0.15$  m the expected feed-down to linear detuning increases significantly (due to the larger  $\beta$  functions in the IR magnets), and the relative precision of the feed-down scan measurements increases correspondingly. Figure 10 compares distributions, over another 6000 simulated scans at  $\beta^* = 0.15$  m, of the true linear and quadratic variations with crossing-angle (pale blue) to distributions

**Fig. 10** Histograms of expected linear (left) and quadratic (right) variations of the vertical direct detuning coefficient as a function of the crossing-angle in IR5, for models of the HL-LHC at  $\beta^* = 0.15$  m (pale blue). The difference between the modelled linear and quadratic variations and those determined from artificial crossing-scan measurements are shown in dark blue

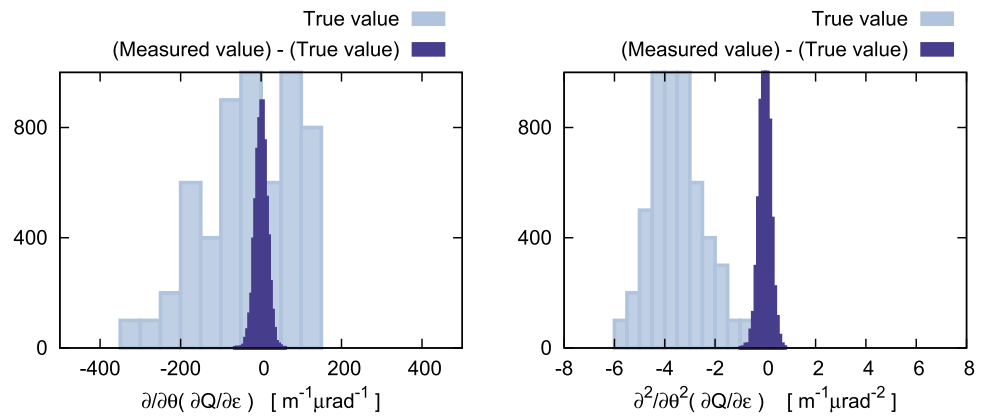
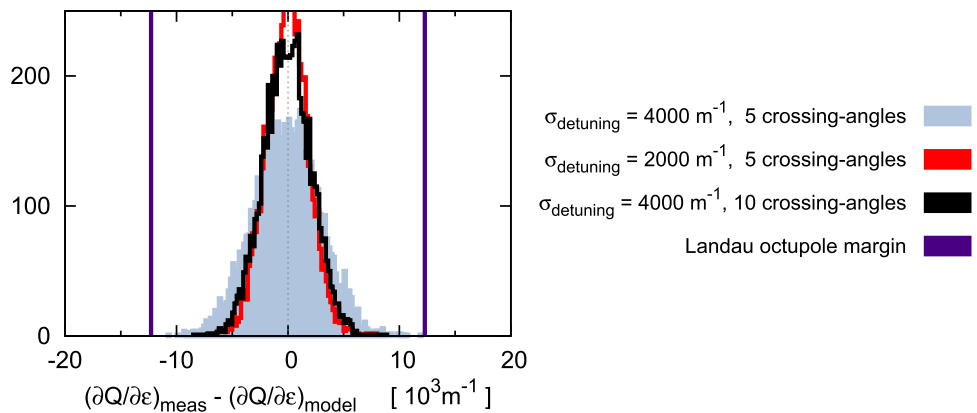


**Fig. 11** Difference obtained at  $\beta^* = 0.4$  m,  $190 \mu\text{rad}$ , between the direct detuning value via fits to simulated measurement of detuning vs crossing-angle, versus the true value obtained from the model. A histogram is shown for simulated crossing-scan measurements with detuning measurements at 5 individual crossing-angles and applied random detuning errors of  $\sigma_{\text{detuning}} = 4000 \text{ m}^{-1}$  (blue) and  $\sigma_{\text{detuning}} = 2000 \text{ m}^{-1}$  (red). A histogram is also shown for simulated crossing-scan measurements with detuning measurements at 10 individual crossing-angles and applied random detuning errors of  $\sigma_{\text{detuning}} = 4000 \text{ m}^{-1}$  (black)



of the measurement discrepancy (dark blue). At this smaller  $\beta^*$  precision is sufficient to study both the decapole and dodecapole components of the feed-down.

While improved precision of the crossing-angle scans can be obtained by going to smaller  $\beta^*$ , measurement at  $\beta^* \approx 0.4$  m will still be of interest in the initial years of HL-LHC operation (before the full  $\beta^*$ -reach of the HL-LHC is achieved). Of particular concern is whether the feed-down can be measured with good precision compared to the tolerance on residual amplitude detuning defined by available margin in the Landau octupoles, as presented in Sect. 3 ( $12 \times 10^3 \text{ m}^{-1}$ ). To assess this, fitted polynomial terms from the 6000 simulated scans at  $\beta^* = 0.4$  m, were used to infer the detuning value at a crossing-angle of  $190 \mu\text{rad}$  and  $\beta^* = 0.4$  m. Figure 11 shows the discrepancy between the true direct detuning terms and those obtained from simulated crossing-angle scans.

The precision of detuning variation with feed-down inferred from the simulated crossing-angle scans is equivalent to  $\approx 10 \times 10^3 \text{ m}^{-1}$  in the worst cases, which is within the available detuning margin, and is significantly better than the level at which detuning was observed to impact on performance of beam instrumentation (as discussed in Sect. 3). In the assumption of random measurement errors better precision could also be achieved via reduction in the uncertainty on the individual detuning measurements (Fig. 11, red), which considering Fig. 7 represents an optimistic but achievable target, and by increasing the number of scanned crossing-angles (Fig. 11, black).

A potential weakness of this method is that to measure feed-down to linear detuning vs crossing-angle multiple high-quality detuning measurements are necessary. Detuning measurements such as that seen in black in Fig. 6 necessitate many AC-dipole excitations. In the mentioned example about 20 kicks were performed at varying amplitudes, taking between 30 – 60 minutes. Scaling this to a realistic HL-LHC measurement scenario would constitute a significant investment of beam-time (approximately 800 kicks, requiring 20–40 hours of measurements [22, 34]).

LHC experience has shown that high-quality detuning measurements using forced oscillations with an AC-dipole could be consistently obtained even with large crossing-schemes applied, and measurement of feed-down to linear detuning coefficients in experimental insertions has been demonstrated at top-energy. On the basis of this LHC experience measurement of feed-down to the linear detuning does appear to be a viable observable to quantitatively study the nonlinear errors up to dodecapole order in the HL-LHC.



**Fig. 12** Example of tune spectrum obtained from a large amplitude AC-dipole excitation in the LHC at  $\beta^* = 0.3$  m, showing visible spectral components corresponding to normal and skew decapole resonances, highlighted in orange and pink, respectively

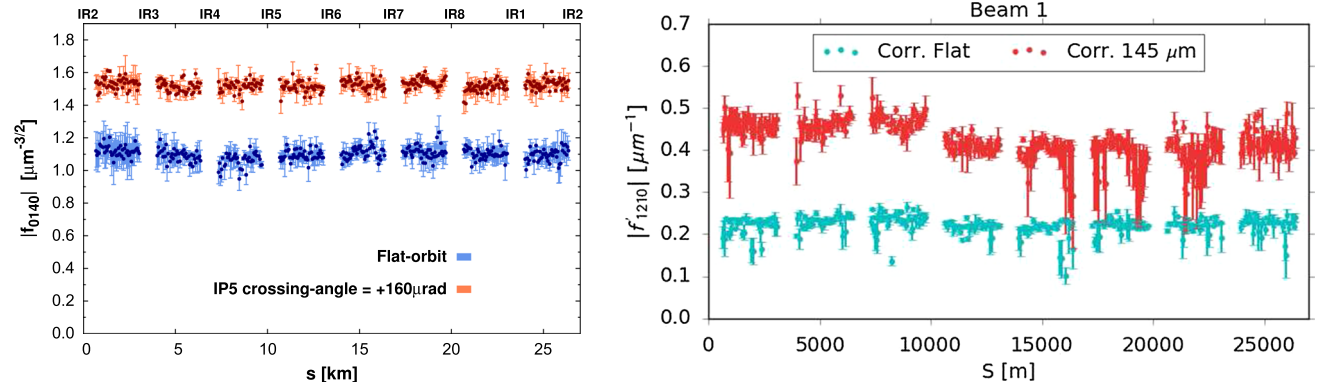
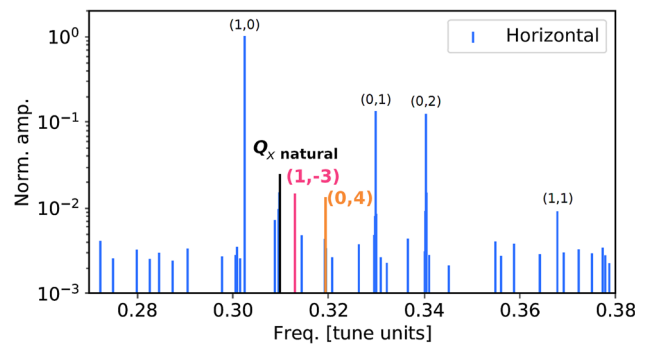


**Fig. 13** Left: measurement of forced decapole RDT  $|f_{0140}|$  performed during 2022 LHC commissioning at  $\beta^* = 0.3$  m. Measurements were performed for flat-orbit (blue) and with a  $-160 \mu\text{rad}$  horizontal crossing-angle orbit bump applied only in IR5 (red). Right: measurement of forced skew-octupole RDT  $f_{1210}$  performed during dedicated machine tests in 2018 at  $\beta^* = 0.3$  m. Measurements were performed for flat-orbit (teal) and with a  $145 \mu\text{rad}$  crossing-scheme applied in IR1 and IR5 (red)

### 5 Resonance driving terms (RDT)

Baseline correction strategy for nonlinear errors in LHC and HL-LHC experimental IRs assumes local minimisation of selected resonances [6, 17, 46, 47]. The prospect for direct beam-based measurement and correction of resonance driving terms (RDT) is therefore of interest. Measurement via the conventional approach (spectral analysis following single-kicks) is not viable at top-energy in LHC or HL-LHC due to restrictions from machine protection (relating to the risk of a superconducting magnet quench), limits from available kicker strength, and practical limitations due to the decoherence of the bunches following single kicks [18, 34]. ‘Forced RDTs’ of oscillations driven with the AC-dipole however, can be considered [36, 48]. Such AC-dipole-based measurements have been employed extensively in the LHC to validate sextupole and octupole corrections [12], and to directly determine skew-octupole corrections [48]. A review of the methodology for AC-dipole based RDT measurement in the LHC is provided in [48].

Dodecapole RDTs have never been successfully identified or measured in beam-based studies of the LHC. This includes occasions where  $b_6$  was enhanced to generate perturbations on a scale anticipated at HL-LHC end-of-squeeze (such as the quadratic detuning studies in Sect. 4.1, and [49]). Without significant hardware improvements (for example reductions to BPM noise, or upgrades to increase AC-dipole excitation length and maximum amplitude) it does not appear viable to measure dodecapole RDTs with existing measurement procedures.

Forced normal- and skew-decapole RDTs were, however, measured for the first time in the LHC at top-energy in 2018 [48]. Figure 12 shows an example of the horizontal spectrum obtained from large amplitude AC-dipole kicks in the LHC at  $\beta^* = 0.3$  m (for non-colliding beams, with no enhanced error sources). Spectral lines corresponding to normal decapole RDT  $f_{1004}$  and skew decapole RDT  $f_{1130}$  can be identified at frequencies  $(0, 4Q_y)$  (highlighted in orange) and  $(Q_x, -3Q_y)$  (highlighted in pink), respectively. The spectral line corresponding to the tune of the free oscillation is shown in black.

The crossing-scheme in the experimental insertions of the HL-LHC may generate feed-down from normal- and skew-dodecapole errors to RDTs of lower-order multipoles. In fact, changes to octupole and decapole forced RDT strength with crossing-angle have already been observed in the LHC. Figure 13 (left) shows measurements of the forced normal-decapole RDT  $|f_{0140}|$  at flat-orbit (blue) and with a horizontal crossing-angle ( $-160 \mu\text{rad}$ ) introduced in the IR5 (CMS) insertion (red). Figure 13 (right) shows measurements of the skew-octupole RDT  $f_{1210}$  at flat-orbit and with  $145 \mu\text{rad}$  crossing-angles applied in both the ATLAS (IR1) and CMS (IR5) insertions. Forced RDT amplitude is plotted for BPMs in the LHC arcs, and feed-down to linear coupling and tune were corrected between measurements at flat-orbit and with crossing-angles applied.

**Table 3** Minimum RDT amplitudes successfully measured in LHC, and typical measurement uncertainties, for selected skew-octupole, skew-decapole, and normal decapole RDTs

Multipole	Minimum $ f_{jklm} $ measured	Typical measurement uncertainty
Skew-octupole ( $f_{1210}$ )	$0.1 \mu\text{m}^{-1}$	$0.02 \mu\text{m}^{-1}$
Skew-decapole ( $f_{0014}$ )	$0.35 \mu\text{m}^{-3/2}$	$0.05 \mu\text{m}^{-3/2}$
Normal-decapole ( $f_{0140}$ )	$0.9 \mu\text{m}^{-3/2}$	$0.05 \mu\text{m}^{-3/2}$

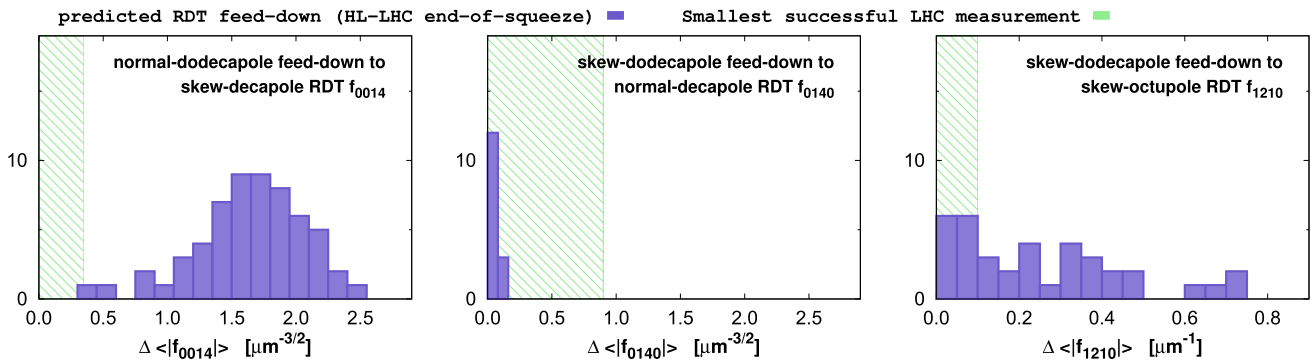


**Fig. 14** Predicted feed-down to selected RDTs in the HL-LHC at  $\beta^* = 0.15$  m, upon introduction of a  $250 \mu\text{rad}$  vertical crossing-angle in the IR5 (CMS) insertion. Values shown are the change in mean RDT amplitude in the arc BPMs, compared to the value expected at flat-orbit. Histograms are shown over sixty seeds of the magnetic model to account for uncertainty in the expected errors. Plots show feed-down from skew-dodecapole errors to normal-decapole RDT  $f_{0140}$  (left), feed-down from normal-dodecapole errors to skew-decapole RDT  $f_{0014}$  (centre), and feed-down from skew-dodecapole errors to skew-octupole RDT  $f_{1210}$  (right). For each RDT the smallest amplitude measured in the LHC at top energy is shown (green)

Skew-octupole and decapole-order RDTs have now been measured on multiple occasions in the LHC at top-energy. Table 5 in Appendix A summarises amplitudes and uncertainties of relevant forced RDT measurements from the LHC in 2018 [48] and 2022. Based on this experience, Table 3 details minimum RDT amplitudes successfully measured to date and gives estimates for achievable RDT measurement uncertainties.

Figure 14 shows the predicted feed-down from dodecapole-order errors to selected lower-order RDTs, expected in the HL-LHC at end-of-squeeze, due to introduction of a  $250 \mu\text{rad}$  vertical crossing-angle in the IR5 (CMS) insertion (sixty seeds of the magnetic model are considered). Similar results are obtained for the IR1 (ATLAS) insertion.

With a vertical crossing-angle in IR5, normal-dodecapole errors feed-down linearly to skew-decapole RDTs. The expected feed-down to  $|f_{0014}|$  (Fig. 14, left) is significant compared to both the minimum RDT amplitude successfully measured in the LHC, and compared to the typical uncertainty on the RDT measurement detailed in Tab. 3. By contrast the expected feed-down from skew-dodecapole errors to normal-decapole RDTs (Fig. 14, center) is small in comparison with the successfully measured decapole RDTs and uncertainties. Interestingly, however, the expected feed-down from skew-dodecapole errors to skew-octupole RDT  $f_{1210}$  (Fig. 14, right) is, for many seeds of the magnetic model, significant in comparison with the minimum amplitude measured and to the typical measurement uncertainty (skew-octupole RDTs are considerably more easily measured in the LHC than decapole RDTs).

Figure 15 shows two examples of simulated measurements of RDT feed-down in the HL-LHC at  $\beta^* = 0.15$  m. Feed-down is shown as a function of vertical crossing-angle in the CMS (IR5) insertion, from normal-dodecapole errors to skew-decapole RDT  $f_{0014}$  (Fig. 15, left) and from skew-dodecapole errors to skew-octupole RDT  $f_{1210}$  (Fig. 15, right). The true variation of the RDT with crossing-angle in the model (dark blue) is obtained from PTC simulations. Corrections for octupole- and decapole-order errors were applied in the model, and tune and coupling were corrected at each crossing-angle. RDT values quoted are the mean amplitudes in the arc BPMs. Simulated measurements (red) were generated in  $20 \mu\text{rad}$  steps, by adding random Gaussian errors to the true model values, with  $\sigma_{|f_{jklm}|}$  defined as in Table 3 (truncated to  $3\sigma$ ). Errors on the crossing-angle were taken to be  $\sigma_\theta = 10 \mu\text{rad}$  (truncated at  $3\sigma$ ) as in Sect. 4.2.

Linear and quadratic variations of the decapole and skew-octupole RDTs due to feed-down can be clearly seen in Fig. 15 left and right, respectively. In Fig. 15 (left) grey lines indicate the feed-down expected upon changing the systematic normal-dodecapole component of the HL-LHC triplets by  $\Delta b_6 = \pm 0.5$  units (relative to the original systematic  $b_6 = -4$  units). In Fig. 15 (right) grey lines represent the feed-down expected due to changing the systematic skew-dodecapole component of the triplets by  $\Delta a_6 = \pm 0.3$  units.

Figures 14 and 15 imply that, based on the quality of forced skew-octupole and decapole-order RDTs which have been achieved in the LHC so far, it should be possible to measure feed-down to such RDTs from normal- and skew-dodecapole errors in the HL-LHC at end-of-squeeze. Beam-based tests of this subject are currently less advanced than the detuning-based methods presented in the previous section, but represent a promising topic for further development in the future LHC operational runs.

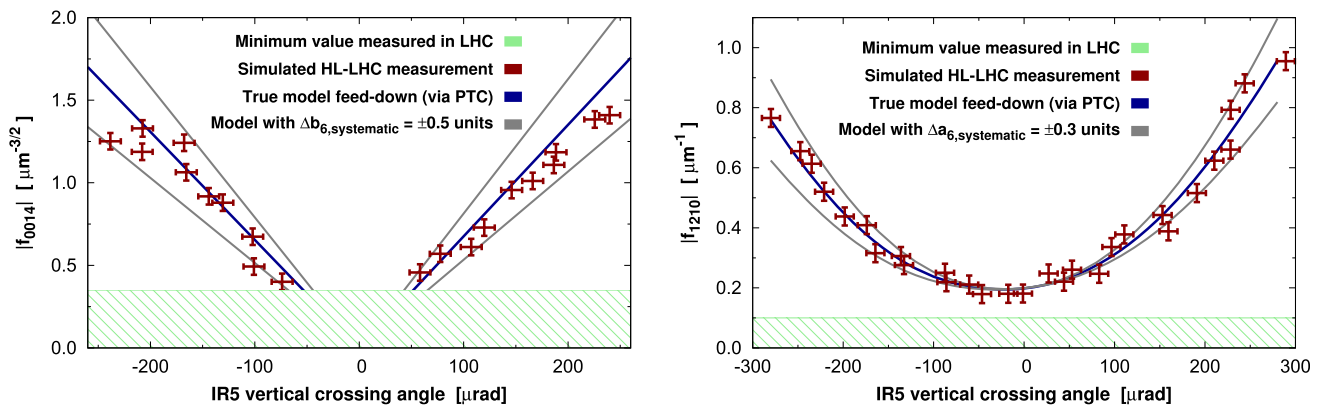


**Fig. 15** Simulated measurements (in the HL-LHC at  $\beta^* = 0.15$  m) of linear feed-down from normal-dodecapole errors to skew-decapole RDT  $f_{0014}$  as a function of vertical crossing-angle in the IR5 insertion (left), and of quadratic feed-down from skew-dodecapole errors to skew-octupole RDT  $f_{1210}$  (right). RDT values shown are the mean amplitude in the arc BPMs

### 6 Direct measurement of dynamic aperture

Given its close relationship to lifetime [50] (and hence delivered luminosity) dynamic aperture represents a key figure of merit for high-order nonlinear correction in HL-LHC. As such direct measurement of DA is of significant interest to the HL-LHC commissioning. Direct DA measurement could be particularly useful as a means to validate dodecapole corrections determined from the magnetic model or via other beam-based observables: for example, by confirming DA reduction upon removal of the corrections, or as a means to directly benchmark the magnetic model by comparing the measurements to tracking simulations.

During its first two Runs significant experience of direct DA measurement was obtained in the LHC. Conventionally DA measurements have been performed in the LHC at injection, based upon analysis of beam-losses following large amplitude single kicks, with results being found to agree well to that predicted by the LHC model, within about 10% [38]. Unfortunately single-kick based study of DA is not viable at top-energy due to strength requirements in the kicker and the risk of quenching the superconducting magnets. An alternative technique was demonstrated at LHC injection however [51], based upon controlled blow-up of a pilot-bunch to large emittance using noise generated in the transverse damper (ADT), followed by examination of beam-losses upon changes in the nonlinear corrector circuits. The method showed a similar level of agreement ( $\approx 10\%$ ) to model predictions as the kick-based technique [51].

Dedicated beam-tests were therefore performed in the LHC in 2017 to test the viability of using this latter technique to directly measure changes in dynamic aperture due normal dodecapole errors, on the scale expected in HL-LHC at end-of-squeeze. At a  $\beta^* = 0.4$  m, the  $b_6$  correctors in the ATLAS and CMS insertions were used to introduce a large dodecapole perturbation, representative of that expected in the HL-LHC at  $\beta^* = 0.15$  m. Such a procedure mirrors one potential use case for this observable in HL-LHC: introduction of the enhanced dodecapole source in the LHC (via the IR correctors) proxies removal of a  $b_6$  correction at end-of-squeeze in HL-LHC. If a DA reduction can be measured due to the enhanced dodecapoles in the LHC, it implies that a comparable  $b_6$  correction can also be tested in HL-LHC via direct DA measurement. In practice the enhanced dodecapole sources in the LHC at  $\beta^* = 0.4$  m were scaled to generate a quadratic detuning of  $|\partial^2 Q/\partial \epsilon^2| = 6.8 \times 10^{12} \text{ m}^{-2}$ , which is representative of that expected in HL-LHC at end-of-squeeze (Fig. 4).

To measure the impact of the introduced  $b_6$  sources on dynamic aperture, three low-intensity bunches were initially blown-up with the transverse damper to very large normalised emittance of  $\epsilon \approx 25 \mu\text{m}$  in either the horizontal, vertical, or horizontal and vertical planes (the nominal LHC normalised emittance is  $\epsilon = 3.75 \mu\text{m}$ ). The enhanced dodecapole sources in the ATLAS and CMS insertions were then applied and resulting beam-losses measured over an extended period (about 1 hour). The tests were performed with non-colliding beams at flat-orbit (limiting any feed-down from the introduced  $b_6$ ), and with linear optics and lower-order nonlinear errors corrected. More detailed discussion of the measurement procedure is provided in [22, 52] and a discussion of the outcome of the measurements in the context of tests of a diffusion model for DA evolution is also provided in [53].

In the absence of the enhanced  $b_6$  sources (and with lower-order errors well corrected) the dynamic aperture was predicted to lie outside of the collimator aperture. During blow-up of the bunch emittances, prior to application of the enhanced  $b_6$ , losses were observed due to scraping on the collimator aperture, but no persistent losses associated with DA were seen [52], consistent with the model prediction.

Upon application of the enhanced  $b_6$ , clearly measurable beam-losses could be observed due to reduction of the DA. The losses were observed to persist for more than 1 hour following completion of the dodecapole corrector trims (up to the end of the fill), and the evolution of the loss-rate was characteristic of the expected laws for DA evolution with time [54–56]. Figure 16 shows bunch intensity measured during introduction of the enhanced  $b_6$  sources for a bunch blown up in both horizontal and vertical planes (left). The evolution of the surviving fractional intensity following the dodecapole corrector trim is also shown (right).

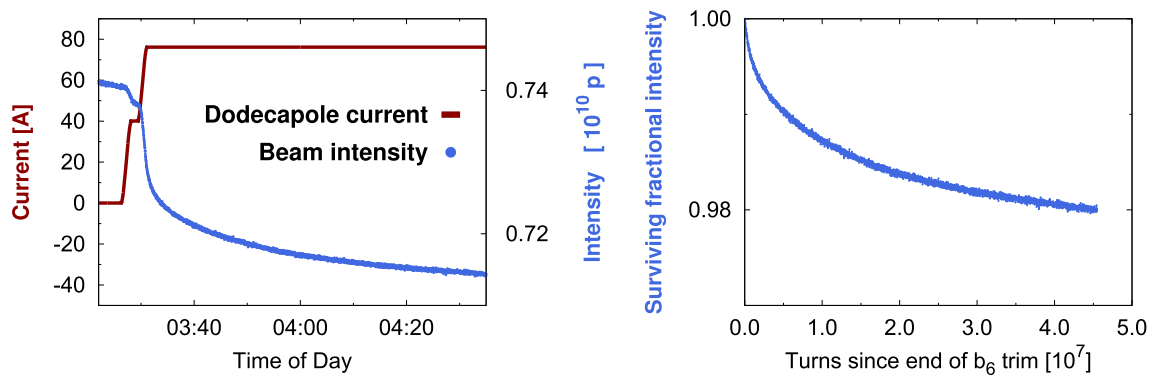
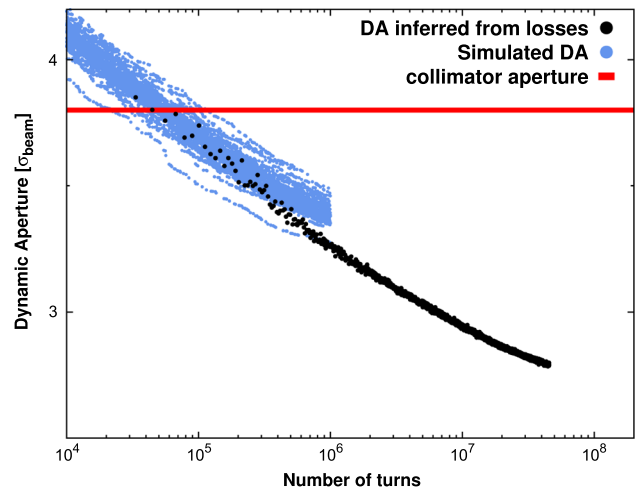


**Fig. 16** Measurement of beam-intensity of bunch with  $\epsilon_x = \epsilon_y \approx 25 \mu\text{m}$  as dodecapole correctors in the ATLAS and CMS insertions are powered on to increase the dodecapole perturbation at  $\beta^* = 0.4 \text{ m}$  to a level representative of that expected in the HL-LHC end-of-squeeze. Measured intensity is shown in the left plot, while the right plot shows the evolution of surviving fractional intensity as a function of the number of turns since the end of the dodecapole trim

**Fig. 17** Evolution of DA inferred from measured beam losses, compared to predictions from SixTrack simulations for evolution of average DA vs turns



The surviving bunch intensity following introduction of the enhanced dodecapole sources can be related to DA for a Gaussian charge distribution,  $\rho = e^{-[(x^2/2\sigma_x^2)+(y^2/2\sigma_y^2)]}$ , according to [55],

$$\begin{aligned} \frac{I(N)}{I(0)} &= 1 - \frac{1}{2\pi\sigma_x\sigma_y} \iint_{D(N)}^{\infty} \rho \, dx \, dy \\ &= 1 - e^{-\frac{D(N)^2}{2}} \end{aligned} \tag{4}$$

where  $N$  indicates the turn number,  $D(N)$  (in units of the beam- $\sigma$ ) represents the average DA over the  $(\sigma_x, \sigma_y)$  parameter space as a function of turn number, and over time the DA is expected to decrease towards the limit of long-term stable motion [26]. Figure 17 compares the dynamic aperture measured after introduction of the enhanced  $b_6$  (Fig. 17, black) as a function of time, to the simulated DA (Fig. 17, blue) obtained from SixTrack [57, 58] tracking simulations (sixty different DA simulations are shown corresponding to different seeds of the magnetic model). Tracking is only performed up to  $10^6$  turns due to computational limitations, and the DA is expressed in units of the measured beam- $\sigma$  (which is much larger than the nominal LHC or HL-LHC emittance). A good agreement between the measured and predicted DA was obtained.

Figures 16 and 17 demonstrate that (given an appropriate experimental configuration) compensation/introduction of a dodecapole error representative of those expected in HL-LHC end-of-squeeze, leads to a change in the dynamic aperture which can be directly measured using the proposed method based on controlled blow-up of the beam via the transverse damper. With known dodecapole sources, the DA reduction due to the enhanced  $b_6$  also agreed well with tracking simulations, which further implies that direct DA measurement should allow tests of the HL-LHC magnetic model via comparison to tracking simulations.

Upon closer inspection of the tracking simulations, it was noticed that the majority of the predicted DA reduction due to the enhanced  $b_6$  sources occurred in the vertical plane, while the horizontal DA was largely unaffected by the dodecaipoles. This can be seen in Fig. 18 which shows survival plots obtained from the SixTrack tracking simulations without (left) and with (right) the

**Fig. 18** SixTrack simulation of the  $10^6$  turn LHC DA at  $\beta^* = 0.4$  m without (left) and with (right) artificially enhanced  $b_6$  sources in the ATLAS and CMS insertions. Amplitude is quoted in units of the measured beam- $\sigma$

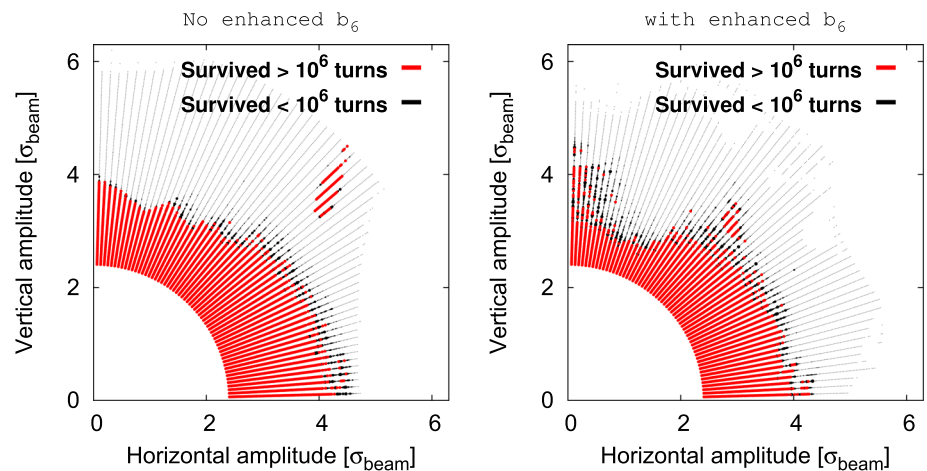
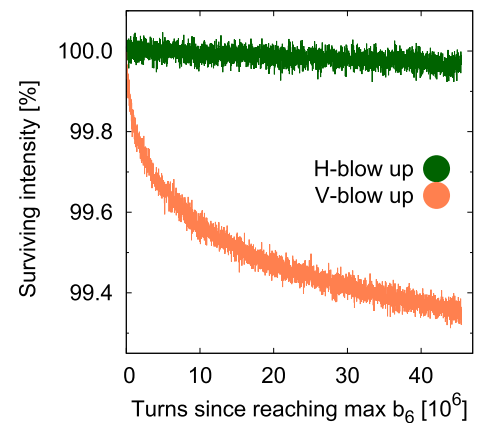


**Fig. 19** Fractional beam-loss observed after introduction of enhanced dodecapole sources in the ATLAS and CMS insertions. Losses are shown for two bunches: one blown-up in only the H plane (green), and one blown-up in only the V plane (orange)



enhanced  $b_6$  sources. Initial conditions which survived  $> 10^6$  turns are shown in red, and amplitude is quoted in units of the measured beam- $\sigma$ . This prediction is reflected in Fig. 19, which compares the surviving fractional intensity of the bunches blown-up only horizontally (green) and only vertically (orange), after introduction of the enhanced dodecapole sources. The pattern of observed losses, with no significant beam-loss from the bunch with large horizontal emittance, but significant losses for the bunch with the large vertical emittance, matches that expected from the model prediction, further demonstrating an ability to probe the impact of dodecapoles on the shape of the DA in the  $(\sigma_x, \sigma_y)$  plane.

While conventional single-kick type DA measurements are not possible at top-energy in the LHC and HL-LHC, the results presented in this section demonstrate that direct dynamic aperture measurement is viable at top-energy based on a method of heating the beam to large emittance with noise from the transverse damper. In particular, deliberately introduced dodecapole sources at the level anticipated in the HL-LHC at end-of-squeeze generated a change in DA which could be clearly measured, and agreed well with predictions of the magnetic model. The measurement procedure utilised in these LHC studies was also straightforward and required relatively little beam time. As such it is of particular interest in regard to rapid validation of dodecapole corrections determined, for example, via magnetic measurements. Ultimately these results also suggest the impact on DA from expected dodecapole errors and correction at HL-LHC end-of-squeeze are large enough to be readily observed, implying direct optimisation of the DA will be a viable option in HL-LHC, and that the magnetic model of the HL-LHC dodecapoles can be benchmarked via direct DA measurement.

### 7 Short-term dynamic aperture of driven oscillations

The DA of a beam under the influence of driven oscillations from an AC-dipole is, in general, substantially smaller than the DA of free betatron oscillations. A discussion of the concept of DA for driven oscillations is provided in [59]. This can pose a challenge to HL-LHC optics commissioning [18], but also provides an observable to test the impact of  $b_6$  errors and their corrections. To test the practicality of the short-term DA of driven oscillations as an observable for the  $b_6$ , dedicated beam-based tests were performed in the LHC at 6.5 TeV. Beam-losses upon excitation for ten thousand turns with an AC-dipole were examined as a function of the AC-dipole kick amplitude, for configurations of the LHC at  $\beta^* = 0.4$  m with and without an enhanced configuration of the  $b_6$  sources which replicated the  $b_6$  perturbation expected in HL-LHC end-of-squeeze. The same enhanced  $b_6$  sources were used for this study as for the free-DA tests described above. A detailed review of the measurements are provided in [52].

**Fig. 20** Measured beam-losses upon AC-dipole excitation with (red) and without (green) artificially enhanced  $b_6$  sources in the ATLAS and CMS insertions of the LHC at  $\beta^* = 0.4$  m. Solid lines show the beam-loss expected for a single-Gaussian profile with  $DA_{forced}$  equal to  $2.8 \sigma_{nom}$  and  $3.3 \sigma_{nom}$  for configurations with and without the enhanced  $b_6$ , respectively

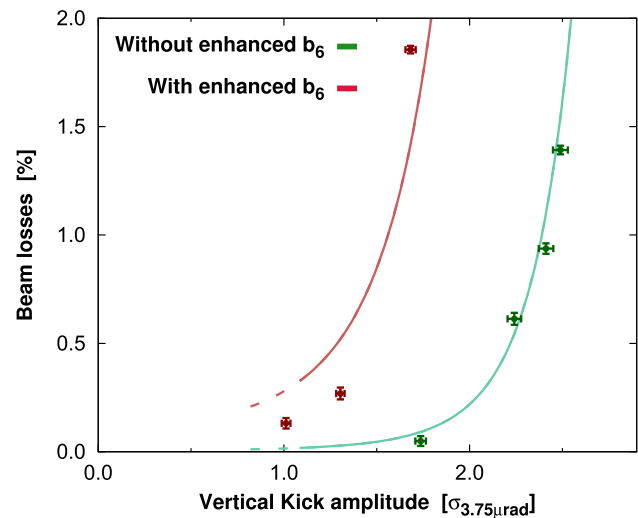


**Table 4** Measured DA of driven oscillations before and after application of  $b_6$  sources representative of those expected in HL-LHC end-of-squeeze

Configuration	DA
Without enhanced $b_6$	$2.8 \sigma_{nom}$
With enhanced $b_6$	$3.3 \sigma_{nom}$

Figure 20 shows measured beam losses upon AC-dipole excitation with (red) and without (green) the enhanced  $b_6$  sources. A clearly measurable increase to the beam-losses can be observed in the enhanced  $b_6$  configuration (for unchanged emittance). This demonstrates that  $b_6$  sources representative of those expected in HL-LHC end-of-squeeze can lead to a measurable shift in the short-term DA of driven oscillations.

An expression for beam-losses upon AC-dipole excitation as a function of the action of the forced-DA and kick is given in Eq. (14) of [59], which can be used to infer the DA by minimisation of the residual to data in Fig. 20. The resulting DA before and after application of the enhanced  $b_6$  sources is shown in Table 4.

The forced DA does not directly relate to that of free-betatron oscillations due to the different detuning pattern and the presence of additional resonances of the driven motion [59]. As such it does not provide an alternative to direct measurement of the dynamic aperture of free oscillations. Nonetheless, since dedicated tests in the LHC imply that dodecapole compensation in HL-LHC at end-of-squeeze should lead to measurable changes in the DA of driven oscillations, it represents an additional observable which can provide qualitative information regarding the quality of  $b_6$  corrections in the HL-LHC.

## 8 Conclusions

The prospect for beam-based study of high-order nonlinear errors, up to dodecapole order, is a topic of significant and immediate interest to the High-Luminosity upgrade of the LHC, as well as of more general interest to the accelerator community in the context of future collider projects. It also represents an intensely challenging topic within the field of beam-optics, particularly at high-energy where many conventional measurement techniques for the nonlinear dynamics cannot be applied. Looking forwards, specifically to the HL-LHC era, it is important to understand whether beam-based measurement of the dodecapole errors can be assumed to be feasible, and if so which techniques are of interest. Such conclusions will inform not only development of theoretical studies, but also the commissioning strategy. Although challenging, multiple beam-based measurement techniques have been identified which, based upon real-world experience in the LHC, appear viable options to use during the optics commissioning of the HL-LHC.

Detuning-based methods show significant potential. Measurement of quadratic tune change with the action of AC-dipole kicks was demonstrated in the LHC at top-energy, and a precision around 20% was achieved for a  $b_6$  perturbation representative of that expected at HL-LHC end-of-squeeze. LHC experience also demonstrated that high-quality measurements of the change to linear detuning coefficients with crossing-angle due to feed-down can be achieved with the AC-dipole at top-energy. Based upon achievable quality of the linear detuning measurements in the LHC, measurement of feed-down to linear detuning during crossing-angle scans in the experimental IRs represents a viable observable for the HL-LHC, even at  $\beta^*$  as high as 0.4 m, before the ultimate  $\beta^*$ -reach has been achieved.

In contrast it has never proved possible to identify spectral lines corresponding to dodecapole RDTs in the LHC, even where dodecapole perturbations (representative of those expected at HL-LHC end-of-squeeze) have been artificially introduced. Consequently, direct RDT measurement appears unlikely to be a viable observable for dodecapole errors without significant hardware

improvements. Robust measurements of forced skew-octupole and normal- and skew-decapole RDTs have been achieved with AC-dipole excitation at top energy in the LHC, however. Under the influence of changes in crossing-angle in the experimental IRs, feed-down from normal-dodecapole errors is predicted to give shifts in decapole RDTs which are significant compared to typical measurement uncertainties achieved already in the LHC. Similarly the feed-down from skew-dodecapole errors to skew-octupole RDTs is also expected to be measurable in HL-LHC at end-of-squeeze. This is of particular interest since few quantitative beam-based observables exist for skew-dodecapole sources. RDT methods have been less thoroughly tested in the LHC compared to detuning-based techniques, and further development and testing will be a priority during the next operational run.

Finally, direct measurement of changes to dynamic aperture have also been demonstrated in the LHC at 6.5 TeV, under the influence of normal dodecapole perturbations representative of those anticipated in HL-LHC at end-of-squeeze. Demonstrations were achieved for both the long-term DA of free betatron-oscillations, via heating of bunch emittance with the transverse damper, and for the short-term DA of forced oscillations under the influence of an AC-dipole. Both methods are comparatively straightforward and fast to employ. As such, they represent a promising tool for the rapid validation of corrections based upon magnetic measurements or even a direct optimisation. This is significant as the DA represents an important figure of merit for operation of the collider at end-of-squeeze.

**Acknowledgements** The authors' copious thanks go to the CERN Operations Group and LHC Operators and Engineers in Charge for the significant amount of support lent to the beam-based studies presented here. Similarly, deep thanks go to the LHC Collimation team and CERN Beam Instrumentation Group without who's work none of the methods presented in this paper would be viable. We are deeply indebted to the CERN Magnets, Superconductors, and Cryostats Group for their extensive work on the magnetic models of both the LHC and HL-LHC, which underpins all the studies presented here. Great thanks also go to the LHC Optics Measurement and Correction team for their broad support of the beam-based optics studies in the LHC.

Dynamic aperture simulations presented in this paper were performed using the LHC@home citizen computing project. The LHC@home volunteers are warmly thanked for the CPU-time they have donated to the project, which is essential to facilitate the large scale tracking studies needed to study dynamic aperture in the HL-LHC.

**Funding** Open access funding provided by CERN (European Organization for Nuclear Research).

**Data Availability Statement** This manuscript has associated data in a data repository. [Authors' comment: The datasets generated and analysed in this manuscript are available upon reasonable request, by contacting the corresponding author.]

**Open Access** This article is licensed under a Creative Commons Attribution 4.0 International License, which permits use, sharing, adaptation, distribution and reproduction in any medium or format, as long as you give appropriate credit to the original author(s) and the source, provide a link to the Creative Commons licence, and indicate if changes were made. The images or other third party material in this article are included in the article's Creative Commons licence, unless indicated otherwise in a credit line to the material. If material is not included in the article's Creative Commons licence and your intended use is not permitted by statutory regulation or exceeds the permitted use, you will need to obtain permission directly from the copyright holder. To view a copy of this licence, visit <http://creativecommons.org/licenses/by/4.0/>.

## A Summary of successful skew-octupole and decapole-order RDT measurements in the LHC

Skew-octupole and normal- and skew-decapole forced RDTs have been successfully measured on several occasions in the LHC at top energy. Table 5 summarises measured amplitudes and uncertainties of relevant forced RDT measurements performed in the LHC at top energy in 2018 (detailed discussion of Run 2 studies can be found in [48]) and 2022.

**Table 5** Summary of successful measurements of skew-octupole, normal-decapole and skew-decapole forced RDT in the LHC at top-energy. RDT values quoted are the mean and standard deviation amplitudes over all BPMs in the LHC arcs

RDT	Multipole	$\langle  f_{jklm}  \rangle_{\text{BPM}} [\mu\text{m}^{-1}]$	$\sigma_{ f_{jklm} } [\mu\text{m}^{-1}]$
$f_{1210}$	$a_4$	0.38	0.01
$f_{1210}$	$a_4$	0.46	0.02
$f_{1210}$	$a_4$	0.10	0.02
$f_{1210}$	$a_4$	0.530	0.008
$f_{1210}$	$a_4$	0.349	0.005
$f_{1210}$	$a_4$	0.54	0.01
RDT	Multipole	$\langle  f_{jklm}  \rangle_{\text{BPM}} [\mu\text{m}^{-3/2}]$	$\sigma_{ f_{jklm} } [\mu\text{m}^{-3/2}]$
$f_{1004}$	$b_5$	1.09	0.09
$f_{1004}$	$b_5$	1.30	0.02
$f_{0140}$	$b_5$	0.90	0.05
$f_{0140}$	$b_5$	1.21	0.04
$f_{0140}$	$b_5$	1.10	0.04
$f_{0140}$	$b_5$	1.33	0.03
$f_{0140}$	$b_5$	1.52	0.03
$f_{0014}$	$a_5$	0.35	0.03
$f_{0014}$	$a_5$	5.31	0.05
$f_{1130}$	$a_5$	5.1	0.1

## References

- I. Béjar Alonso, O. Bruning, P. Fessia, M. Lamont, L. Rossi, L. Tavian, M. Zerlauth, High-Luminosity Large Hadron Collider (HL-LHC): Technical design report. Technical report, (2015). CERN-2020-010
- J. Coupard, H. Damerau, A. Funken, R. Garoby, S. Gilardoni, B. Goddard, K. Hanke, A. Lombardi, D. Manglunki, M. Meddahi, B. Mikulec, G. Rumolo, E. Shaposhnikova, M. Vretena, (eds.), LHC Injectors Upgrade, Technical Design Report. CERN, (2014)
- L.C. Teng, Error analysis for the low- $\beta$  quadrupoles of the Tevatron collider. Technical report (1982). FERMILAB-TM-1097
- J. Wei, M. Harrison, The RHIC project - design, status, challenges, and perspectives. In Multi-GeV high-performance accelerators and related technology. Proceedings, 16th RCNP International Symposium, Osaka, Japan, March 12-14, 1997, number C97-03-12.1 p.198-206, (1997). FERMILAB-TM-1097
- O. Brüning et al. (eds.), LHC Design Report v.1: the LHC Main Ring. CERN (2004)
- J. Wei, W. Fischer, V. Ptitsyn, Interaction Region Local Correction for the Large Hadron Collider. In Proceedings of the 1999 Particle Accelerator Conference, New York (1999)
- H. Grote, F. Schmidt, L.H.A. Leunissen. LHC dynamic aperture at collision. Technical report (1999). LHC-PROJECT-NOTE-197
- O.S. Brüning, S. Fartoukh, M. Giovannozzi, Field quality issues for LHC magnets: analysis and perspectives for quadrupoles and separation dipoles. Technical report (2004). CERN-AB-2004-014-ADM
- F. Pilat, Y. Luo, N. Malitsky, V. Ptitsyn, Beam-based non-linear optics corrections in colliders. In Proceedings of PAC'05, number WOAC007 (2005)
- W. Fischer, J. Beebe-Wang, Y. Luo, S. Nemesure, L. Rajulapati, RHIC proton beam lifetime increase with 10- and 12-pole correctors. In Proceedings of IPAC 2010, number THPE099 (2010)
- J. Koutchouk, F. Pilat, V. Ptitsyn, Beam-based measurements of field multipoles in the RHIC low-beta insertions and extrapolation of the method to the LHC. In Proceedings of the 2001 Particle Accelerator Conference, Chicago (2001)
- E.H. Maclean, R. Tomás, F.S. Carlier, M.S. Camillocci, J.W. Dilly, J.M. Coelho de Portugal, E. Fol, K. Fuchsberger, A. Garcia-Tabares Valdivieso, M. Giovannozzi, M. Hofer, L. Malina, T.H.B. Persson, P.K. Skowronski, A. Wegscheider, New approach to LHC optics commissioning for the nonlinear era. Phys. Rev. Accel. Beams **22**, 061004 (2019)
- D. Schulte, Optics challenges for future hadron colliders. CERN-ICFA Workshop on Advanced Optics Control (2015)
- M. Benedikt, D. Schulte, J. Wenninger, F. Zimmerman, Challenges for highest energy circular colliders. Technical report (2014). CERN-ACC-2014-0153
- E. Cruz-Alaniz, A. Seryi, E.H. Maclean, R. Martin, R. Tomás, Non linear field correction effects on the dynamic aperture of the FCC-hh. In Proc. IPAC 17. Copenhagen, Denmark, number TUPVA038 (2017)
- H. Sugimoto, SuperKEKB. Presentation at CERN-ICFA Workshop on Advanced Optics Control (2015)
- O. Bruning, S. Fartoukh, M. Giovannozzi, T. Risselada, Dynamic Aperture Studies for the LHC Separation Dipoles. Technical report (2004). LHC Project Note 349
- F. Carlier, J. Coelho, S. Fartoukh, E. Fol, A. Garcia-Tabares, M. Giovannozzi, M. Hofer, A. Langer, E.H. Maclean, L. Malina, L. Medina, T.H.B. Persson, P. Skowronski, R. Tomás, F. Van der Veken, A. Wegscheider, Optics Measurement and Correction Challenges for the HL-LHC. Technical report (2017). CERN-ACC-2017-0088
- T. Pugnat, B. Dalena, A. Simona, L. Bonaventur, Computation of beam based quantities with 3D final focus quadrupoles field in circular hadronic accelerators. Nucl Instrum. Methods Phys. Res. Sect. A: Accel. Spectrom. Detect. Assoc. Equip. **978**, 164350 (2020)
- T. Pugnat, 3D magnetic field analysis of LHC final focus quadrupoles with Beam Screen. In Proceedings of IPAC 21, (2021)
- E.H. Maclean, R. Tomás, M. Giovannozzi, T.H.B. Persson, First measurement and correction of nonlinear errors in the experimental insertions of the CERN Large Hadron Collider. Phys. Rev. Spec. Top. Accel. Beams **18**, 121002 (2015)
- E.H. Maclean, F. Carlier, J. Dilly, M. Giovannozzi, R. Tomás, Prospects for beam-based study of dodecapole nonlinearities in the CERN High-Luminosity Large Hadron Collider. Technical report. CERN-ACC-NOTE-2022-0020
- G. Ambrosio, P. Ferracin, MQXF (results of all type of tests and global plan CERN/AUP). Presentation to 7th HL-LHC Collaboration Meeting, CIEMAT, Madrid, 13–16 November (2017)



24. S.I. Bermudez, MQXFB status. Presentation to 10th HL-LHC Collaboration Meeting, CERN, 5–7 October (2020)
25. G. Ambrosio, Results of the US triplet pre-series magnet tests and measurements. Presentation to 10th HL-LHC Collaboration Meeting, CERN, 5–7 October (2020)
26. E. Todesco, M. Giovannozzi, Dynamic aperture estimates and phase-space distortions in nonlinear betatron motion. *Phys. Rev. E* **53**, 4067 (1996)
27. G. Apollinari, I. Béjar Alonso, O. Bruning, M. Lamont, L. Rossi, High-Luminosity Large Hadron Collider (HL-LHC): preliminary Design Report. Technical report. CERN-2015-005
28. M. Giovannozzi, Field quality and DA. 6th HL-LHC Collaboration Meeting (14–16 November 2016, Paris)
29. I. Béjar Alonso, L. Rossi, HiLumi LHC Technical Design Report: Deliverable: D1.10. Technical report. CERN-ACC-2015-0140
30. N. Karastathis, Y. Papaphilippou, Beam-beam simulations for optimizing the performance of the High-Luminosity Large Hadron Collider Proton Physics. Technical report (2020). CERN-ACC-NOTE-2020-0026
31. S. Kostoglou, DA simulations with beam-beam for HL-LHC. 194th HiLumi WP2 Meeting, CERN, 27 July (2021)
32. CERN FiDeL group documentation on the magnetic model of the LHC. Technical report
33. A. Bazzani, E. Todesco, G. Turchetti, A normal form approach to the theory of nonlinear betatronic motion. *CERN* **94**(02), (1994)
34. X. Buffat, F.S. Carlier, J. Coello De Portugal, R. De Maria, J. Dilly, E. Fol, N. Fuster Martinez, D. Gamba, H. Garcia Morales, A. Garcia-Tabares, M. Giovannozzi, M. Hofer, N. Karastathis, J. Keintzel, M. Le Garec, E.H. Maclean, L. Malina, T.H.B. Persson, P. Skowronski, F. Soubelet, R. Tomás, F. Van der Veken, L. Van Riesen-Haupt, A. Wegscheider, D.W. Wolf, J.F. Cardona, Optics Measurement and Correction Strategies for HL-LHC. Technical report (2022). CERN-ACC-2022-0004
35. J. Serrano, M. Cattin, The LHC AC Dipole system: an introduction. Technical report (2010). CERN-BE-Note-2010-014
36. R. Tomás, Normal form of particle motion under the influence of an ac dipole. *Phys. Rev. ST. Accel. Beams* **5**, 054001 (2002)
37. R. Tomás, Adiabaticity of the ramping process of an ac dipole. *Phys. Rev. ST. Accel. Beams* **8**, 024401 (2005)
38. E.H. Maclean, R. Tomás, F. Schmidt, T.H.B. Persson, Measurement of nonlinear observables in the Large Hadron Collider using kicked beams. *Phys. Rev. ST. Accel. Beams* **17**, 081002 (2014)
39. S. White, E. Maclean, R. Tomás, Direct amplitude detuning measurement with ac dipole. *Phys. Rev. ST. Accel. Beams* **16**, 071002 (2013)
40. E.H. Maclean, F.S. Carlier, E. Cruz Alaniz, B. Dalena, J.W. Dilly, E. Fol, M. Giovannozzi, M. Hofer, L. Malina, T.H.B. Persson, J.M. Coello de Portugal, P.K. Skowronski, M.S. Camillocci, R. Tomás, A. Garcia-Tabares Valdivieso, A. Wegscheider, Report from LHC MD 2158: IR-nonlinear studies. Technical report (2017). CERN-ACC-NOTE-2018-0021
41. M. Gasior, R. Jones, The principle and first results of betatron tune measurement by direct diode detection. Technical report (2005). LHC-Project-Report 853
42. A. Boccardi, M. Gasior, O.R. Jones, P. Karlsson, R.J. Steinhagen, First Results from the LHC BBQ Tune and Chromaticity Systems. Technical report (2009). CERN-LHC-Performance-Note-007
43. É. Forest, F. Schmidt, E. McIntosh, Introduction to the Polymorphic Tracking Code. Technical report (2002). CERN-SL-2002-044 (AP)
44. J. Dilly, A. Markus, A. Theodoros, F. Carlier, M. Hofer, L. Malina, E.H. Maclean, E. Solfaroli Camillocci, R. Tomás, Report and Analysis from LHC MD 3311: amplitude detuning at end-of-squeeze. Technical report (2019). CERN-ACC-NOTE-2019-0042
45. J. Dilly, E.H. Maclean, R. Tomás, Controlling Landau Damping via Feed-Down From High-Order Correctors in the LHC and HL-LHC. In Proceedings of the 13th International Particle Accelerator Conference, page WEPOPT060, Bangkok, Thailand (2022). JACoW
46. J. Dilly, R. Tomás, A flexible nonlinear Resonance Driving Term based Correction Algorithm with Feed-Down. In Proceedings of the 13th International Particle Accelerator Conference, page WEPOPT061, Bangkok, Thailand (2022). JACoW
47. J. Dilly, M. Giovannozzi, R. Tomás, F. Van Der Veken, Corrections of Systematic Normal Decapole Field Errors in the HL-LHC Separation/Recombination Dipoles. In Proceedings of the 13th International Particle Accelerator Conference, page WEPOPT059, Bangkok, Thailand (2022). JACoW
48. F.S. Carlier, A Nonlinear Future—Measurements and corrections of nonlinear beam dynamics using forced transverse oscillations. PhD thesis, University of Amsterdam (2020). CERN-THESIS-2020-025
49. J.W. Dilly, M. Albert, F.S. Carlier, J. Coello De Portugal, B. Dalena, E. Fol, M. Hofer, E.H. Maclean, L. Malina, T.H.B. Persson, M.S. Camillocci, M.L. Spitznagel, R. Tomás, A. Garcia Tabares Valdiviesco, Report from LHC MD 3312: Replicating HL-LHC DA. Technical report (2022). CERN-ACC-NOTE-2022-0021
50. M. Giovannozzi, F. Van der Veken, Description of the luminosity evolution for the CERN LHC including dynamic aperture effects. Part II: application to Run 1 data. *Nucl. Instrum. Methods Phys. Res. A* **908**(2018), 1–9, 908 (2018)
51. E.H. Maclean, M. Giovannozzi, R.B. Appleby, Innovative method to measure the extent of the stable phase-space region of proton synchrotrons. *Phys. Rev. Accel. Beams* **22**, 034002 (2019)
52. E.H. Maclean, F.S. Carlier, M. Giovannozzi, R. Tomás, Report from LHC MD 2171: dynamic aperture at 6.5 TeV. Technical report (2018). CERN-ACC-NOTE-2018-0054
53. A. Bazzani, M. Giovannozzi, E.H. Maclean, Analysis of the non-linear beam dynamics at top energy for the CERN Large Hadron Collider by means of a diffusion model. *Eur. Phys. J. Plus* **135**, 77 (2020)
54. M. Giovannozzi, W. Scandale, E. Todesco, Dynamic aperture extrapolation in the presence of tune modulation. *Phys. Rev. E* **57**, 3432 (1998)
55. M. Giovannozzi, Proposed scaling law for intensity evolution in hadron storage rings based on dynamic aperture variation with time. *Phys. Rev. ST. Accel. Beams* **15**, 024001 (2012)
56. M. Giovannozzi, F. Lang, R. de Maria, Analysis of Possible Functional Forms of the Scaling Law for Dynamic Aperture as a Function of Time. Technical report (2013). CERN-ACC-2013-0170
57. SixTrack - 6D Tracking Code. <http://sixtrack-ng.web.cern.ch/SixTrack/index.php>
58. R. De Maria, J. Andersson, V.K. Berglyd Olsen, L. Field, M. Giovannozzi, P.D. Hermes, N. Høimyr, S. Kostoglou, G. Iadarola, E. McIntosh, A. Mereghetti, J. Molson, D. Pellegrini, T. Persson, M. Schwinzler, E.H. Maclean, K.N. Sjobak, I. Zacharov, S. Singh, Sixtrack v and runtime environment. *Int. J. Mod. Phys. A* **34**, 36 (2019)
59. F.S. Carlier, R. Tomás, E.H. Maclean, T.H.B. Persson, First Demonstration of Dynamic Aperture Measurements with an AC dipole. *Phys. Rev. Accel. Beams* **22**, 031002 (2019)